



OPEN ACCESS

EDITED BY

Zhenjiang You,
Edith Cowan University, Australia

REVIEWED BY

Vahid Tavakoli,
University of Tehran, Iran
Ahmed E. Radwan,
Jagiellonian University, Poland

*CORRESPONDENCE

Meiyan Fu,
✉ fumeiyan08@cdu.cn

RECEIVED 18 September 2023

ACCEPTED 26 December 2023

PUBLISHED 12 January 2024

CITATION

Ling C, Zhang X, Fu M, Huang T, Duan G and Gao S (2024), The geological controlling factors of the heterogeneity of a bioclastic limestone reservoir—a case study of the Cretaceous Kh2 layer in A oilfield, Iraq.
Front. Energy Res. 11:1296584.
doi: 10.3389/fenrg.2023.1296584

COPYRIGHT

© 2024 Ling, Zhang, Fu, Huang, Duan and Gao. This is an open-access article distributed under the terms of the [Creative Commons Attribution License \(CC BY\)](https://creativecommons.org/licenses/by/4.0/). The use, distribution or reproduction in other forums is permitted, provided the original author(s) and the copyright owner(s) are credited and that the original publication in this journal is cited, in accordance with accepted academic practice. No use, distribution or reproduction is permitted which does not comply with these terms.

The geological controlling factors of the heterogeneity of a bioclastic limestone reservoir—a case study of the Cretaceous Kh2 layer in A oilfield, Iraq

Can Ling¹, Xiran Zhang¹, Meiyan Fu^{1,2*}, Tingting Huang³, Guanghui Duan¹ and Shumin Gao¹

¹College of Energy, Chengdu University of Technology, Chengdu, China, ²State Key Laboratory of Oil and Gas Reservoir Geology and Exploitation, Chengdu University of Technology, Chengdu, China, ³China Petroleum Formation Chuanqing Drilling Engineering Co., Ltd., Geological Exploration and Development Research Institute, Chengdu, China

Reservoir heterogeneity is one of the key factors affecting the exploration and development of oil and gas reservoirs. The Kh2 layer in the A field of Central Iraq is a major pay zone with strong longitudinal and lateral heterogeneity. The heterogeneity, controlled by geological factors, has not yet been confirmed, which seriously restricts the development of this pay zone. This study aims to establish a geological pattern for the reservoir heterogeneity of bioclastic limestone, providing a geological basis for heterogeneity evaluation. Based on the core observation, thin-section identification, and physical property analysis, the microfacies are classified, and the diagenetic sequences and the pore structure of the Kh2 layer are analyzed. Seven types of microfacies are developed in the Kh2 layer, namely, planktic foraminiferal wackestone (MFT1), lamellar bioclastic wackestone (MFT2), intraclastic–bioclastic packstone (MFT3), green algal packstone (MFT4), green alga–pelletoid packstone (MFT5), bioclastic–intraclastic packstone (MFT6), and intraclastic grainstone (MFT7). The heterogeneity of the different microfacies and heterogeneity within the same microfacies were evaluated using the variation coefficient of permeability tested from cores collected from wells and calculated by well-logging at different intervals. The highest heterogeneity was observed in the lamellar bioclastic wackestone (MFT2), with an average variation coefficient of 0.72. The lowest heterogeneity was observed in the green algal packstone (MFT4), with an average variation coefficient of 0.11. The vertical heterogeneity of the permeability is mainly controlled by sedimentation, while the lateral heterogeneity is mainly influenced by cementation, bioturbation, and the distribution of green algae. Finally, a micro-scale geological pattern for determining the reservoir heterogeneity of bioclastic limestone reservoirs is established. This study can guide the current injection development and remaining oil prediction in oilfields with similar backgrounds.

KEYWORDS

Iraq, limestone, microfacies, heterogeneity, main controlling factors

1 Introduction

The heterogeneity of reservoirs is a key element to evaluate the oil zone, which intensively affects the prediction of the distribution of oil and gas reservoirs. Carbonate reservoirs have relatively higher heterogeneity than sandstone reservoirs, and therefore, heterogeneity evaluation is important for reservoir development (Jodeyri-Agahi et al., 2018; Sharifi-Yazdi et al., 2020; Radwan et al., 2020; Mohammed A. et al., 2022). Reservoir heterogeneity refers to the dispersion degree of various parameters characterizing the reservoir in the three-dimensional space (Chen et al., 2017). Many research studies have reported the main controlling factors of reservoir heterogeneity, especially including original material composition controlled by deposition (Sadooni and alsharhan, 2003; Li et al., 2023) and dissolution and cementation influenced by diagenesis (Nazemi M et al., 2021; Alsuwaidi et al., 2021; Abdel-Fattah et al., 2022; Tavakoli et al., 2022; Khazaie et al., 2022; Mohsin et al., 2023). The lithology of the Cretaceous carbonate reservoir in Iraq is mainly bioclastic limestone with a complex pore type and pore structure. Strong heterogeneity exists in the distribution of particles and vertical variation in pore-type assemblages (Liu et al., 2019), leading to the development of layers with high permeability and interlayers (Elfeki and Dekking, 2001; Sadooni et al., 2004; Han et al., 2014). Meanwhile, strong local bioturbation has also been reported (Shen et al., 2019; Liu et al., 2021). Previous research studies always focused on a single geological factor influencing the heterogeneity of bioclastic limestone in the Middle East (Shen et al., 2019; Wang G. J. et al., 2022; Farouk et al., 2022; Mohammed I. Q. et al., 2022), without the understanding of micro-scale reservoir heterogeneity patterns. Therefore, it is necessary to establish a comprehensive pattern and effective geological heterogeneity model that integrates multiple factors to evaluate the heterogeneity of bioclastic limestone in the study area, in order to provide a favorable foundation for the next injection development and remaining oil prediction of an oilfield.

A oilfield is located in the southeastern part of Iraq. The A oilfield is currently in the water-injection development stage (Han et al., 2014; Khazaie et al., 2022; Mao et al., 2020), and with development, the problem of rapid water-bearing increases, and serious water-injection surges are becoming increasingly apparent. Reservoir heterogeneity is an important factor in the success and efficiency of waterflooding projects (Radwan et al., 2021). The Late Cretaceous Turonian Khasib Formation is one of the major oil-bearing zones in the field (Liu et al., 2019), accounting for 60% of the total reserves of the field. The Kh2 layer has the largest reserves in the Khasib Formation (Xu, 2018). The physical property of the reservoir is mainly controlled by the content of particles and dissolution and cementation (Xu, 2018; Gingras et al., 2014; Chen et al., 2020). The extremely strong heterogeneity of the Kh2 layer reservoir has a serious impact on the field development effect and final recovery (Abdel-Fattah et al., 2022; Xu et al., 2018). In this study, based on the observation of cores and thin sections, the microfacies of the Kh2 reservoir are divided in the A oilfield. Based on the physical property characteristics of the core well, the evaluation method of the reservoir heterogeneity of the horizontal well is established. Through testing and quantitative analysis, the influencing factors of reservoir heterogeneity are analyzed, and then, the heterogeneous development pattern is formed by integrating multiple controlling factors.

2 Geological setting

The A oilfield is structurally located on the south-central Mesopotamian Basin, on the northern edge of the Arabian Plate (Figure 1) (Han et al., 2014; Abdel-Fattah et al., 2022; Wang Q. et al., 2022). The A field is an important oil-producing area (Liu et al., 2019; Wang G. J. et al., 2022). The field is a NE–SW trending broad, gently long-axis anticline. The long axis of the anticline is approximately 50 km long, and the short axis is 15–20 km wide (Sherwani and Aqrabi, 1987). During the late Albian, a carbonate ramp developed in the Mesopotamian Basin. During the early Cenomanian, the base of the Mesopotamian Basin began to rise, forming the inner-shelf basin. During the Turonian, the Khasib Formation began to be deposited. Subsidence of the Mesopotamian Belt occurred at the end of the Permian under the influence of Early Alpine movement. Tectonic activity occurred during the Late Cretaceous Turonian, and then, foreland basin evolution occurred during the Paleoproterozoic–Pliocene, leading to the present tectonic morphology (Guo et al., 2014; Al-Qayim, 2010; Aqrabi, 1997; Zhang et al., 2023).

During the Cretaceous, the study area was weakly tectonically active, depositing massive marine bioclastic-rich carbonate rocks (Khazaie et al., 2022; Al-Qayim, 2010; Haq and Al-Qahtani, 2005; Tian et al., 2020; Xue et al., 2022). Four oil-bearing zones developed in the Cretaceous, namely, the Mauddud Formation, Rumaila Formation, Mishrif Formation, and Khasib Formation, from the bottom to top. Among them, the Khasib Formation is the most important and extensively large oil-producing zone, with reserves accounting for 60% of the total oilfield. The Khasib Formation is unconformable with the Mishrif Formation. The top of the Khasib Formation is underlied by the Tanuma Formation. The Khasib Formation was deposited in the open carbonate platform, including bioclastic shoal and algal mounds (Li et al., 2023; Khazaie et al., 2022; Fadhil, 1993; Guo et al., 2014).

The Khasib Formation can be divided into four layers, Kh1, Kh2, Kh3, and Kh4, and the Kh2 layer in this study is the main oil-producing zone in the study area (Figure 2). The Kh2 layer can be divided into five sub-layers, from Kh2-1 to Kh2-5, from top to bottom (Guo et al., 2014; Zhang et al., 2023; Mahdi and Aqrabi, 2014). The Kh2 layer is characterized by lateral continuity and stable thickness. The analysis of sedimentary microfacies assemblages and sedimentary evolution showed that the Kh2 layer is deposited on the carbonate platform, with the microfacies mainly consisting of intraclastic shoal, bioclastic shoal, algal mound, and inter-bank facies (Mirzaei et al., 2007; Sadooni and Alsharhan, 2003; Xue et al., 2022). The lithology of the Kh2 layer is predominantly grainstone, packstone, and wackestone, containing large amounts of biological debris, foraminifera, and green algae, with minor Echinodermata, bivalves, and gastropods (Mirzaei and Das, 2007; Liu et al., 2019; Shen et al., 2019; Sadooni and alsharhan, 2003; Mao et al., 2020; Gingras et al., 2014).

3 Sampling and testing methods

The cores were collected from a total of seven wells, X-12, X-13, X1-12-8H, X1-22-1H, X-15, X-6, and XMa-4H. A total of 155 thin sections were used in the study, with an interval of 1 m on cores.



Among them, 25 thin sections were collected from well X-12, 24 thin sections were collected from well X-13, 20 thin sections were collected from well X1-12-8H, 26 thin sections were collected from well X1-22-1H, 20 thin sections were collected from well X-15, 23 thin sections were collected from well X-6, and 17 thin sections were collected from well Xma-4H. Based on the observation of cores, the sedimentary textures are identified. Based on the composition and content of particles in the thin sections, the microfacies are classified.

Experimental analysis was carried out at the State Key Laboratory of Oil and Gas Reservoir Geology and Exploitation, China. All thin sections were stained with the alizarin red reagent in 0.2% HCl solution (cold) to differentiate between dolomite and calcite, and impregnated with blue resin under vacuum conditions to characterize the pore structure. Microscopic observations were made using a DM4500 P microscope, and photographs were taken using a Leica microscope. Finally, 155 thin sections were observed and recorded under a microscope with the aim of confirming the rock and mineral composition of the study area.

Based on these samples, the porosities with accuracies of $\pm 0.1\%$ were measured using an UltraPore-300 helium-porosity automatic measuring instrument (Temco, United States), while a PoroPDP-200

gas permeability measuring instrument (Temco, United States) was used to determine the permeability with an accuracy of 0.0001 mD.

The relevant heterogeneity parameters are used to evaluate the heterogeneity of carbonate reservoirs (Shao, 2010). This study focuses on the degree of heterogeneity of permeability, and the heterogeneity evaluation parameters used are as follows:

The variation coefficient (V_k) is defined as $V_k = \frac{\sqrt{\sum_{i=1}^n (K_i - \bar{K})^2 / n}}{\bar{K}}$.

In the formula, K_i is the permeability of the i th test point; n is the number of test points in the study area; and \bar{K} is the average of the permeability, and a weighted average of the thicknesses is usually used in order to reflect the actual situation more objectively.

The dart coefficient (T_k) is defined as $T_k = K_{max} / \bar{K}$, where K_{max} is the maximum value of the permeability in the study area.

The range (J_k) is defined as $J_k = K_{max} / K_{min}$, where K_{min} is the minimum value of the permeability in the study area.

Generally, the larger the above three parameters, the stronger the reservoir heterogeneity; conversely, the weaker it is (Wang and Jing, 2009; Wang et al., 2017). In this study, the heterogeneity of different layers in straight wells and the horizontal sections of horizontal wells were evaluated.

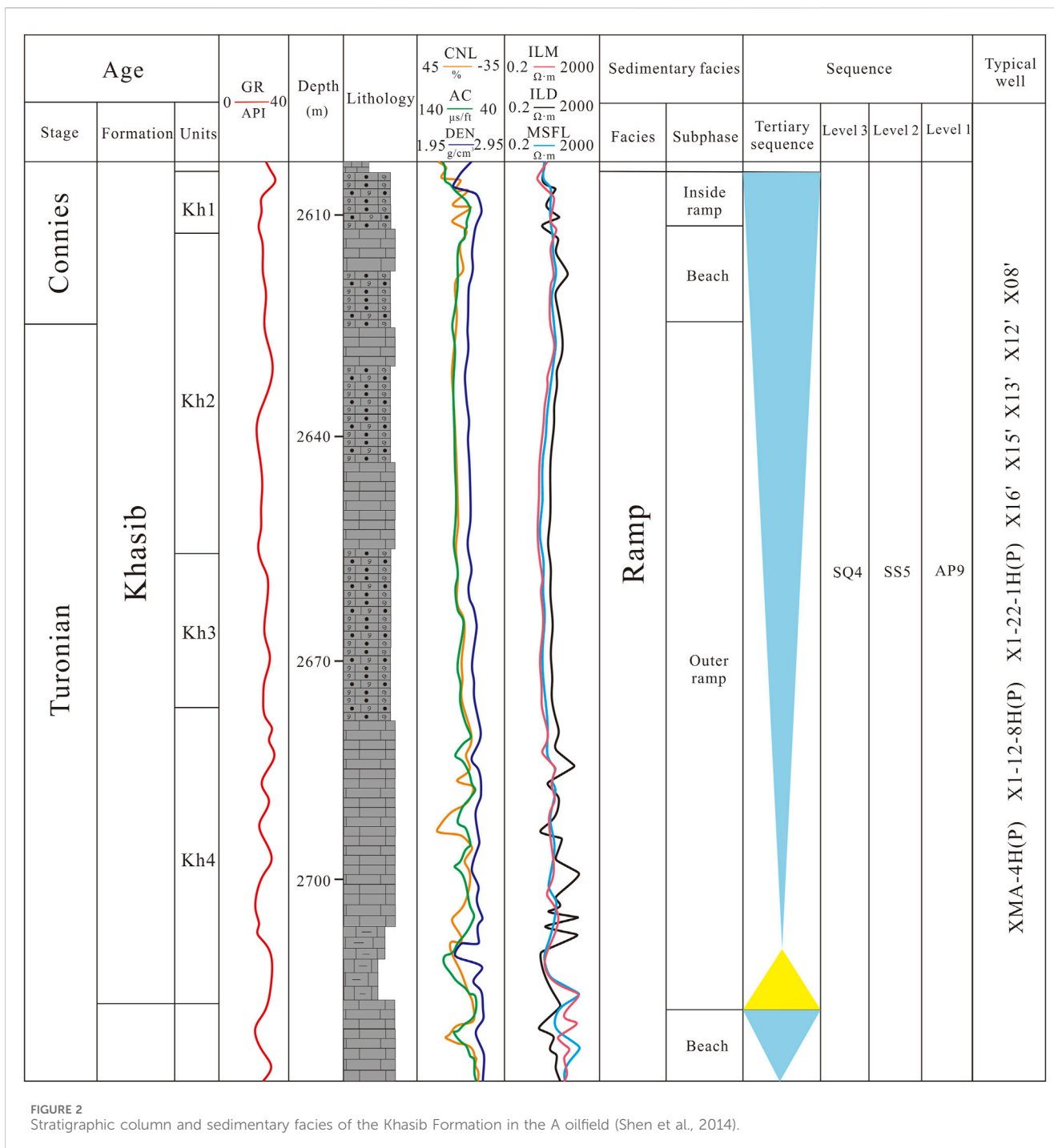


FIGURE 2 Stratigraphic column and sedimentary facies of the Khasib Formation in the A oilfield (Shen et al., 2014).

4 Results

4.1 Microfacies

Based on the carbonate classification criteria (Dunham, 1962), using thin-section identification data and logging data, the microfacies of the Kh2 layer were divided in the study area. Analysis of the logging response characteristics, pore structure, and depositional environment for each type are shown in Table 1, Figure 3, and Figure 4, i.e., planktic foraminiferal wackestone (MFT1) (Figure 3A), lamellar bioclastic wackestone (MFT2) (Figure 3B),

intraclastic–bioclastic packstone (MFT3) (Figure 3C), green algal packstone (MFT4) (Figure 3D), green alga–pelletoid packstone (MFT5) (Figure 3E), bioclastic–intraclastic packstone (MFT6) (Figure 3F), and intraclastic grainstone (MFT7) (Figure 3G). With differences in the grain content, there are different pore assemblies and pore structures among the different microfacies.

The grain type in MFT1 is mainly planktic foraminiferium and contains a small amount of biological debris. The particle content is in the range of 25%–50%. Good pore structures of the microfacies exist, filled with micrite calcite between the grains, with visible porosity in the range of 5%–10%.

TABLE 1 Microfacies characteristics of the Kh2 layer in the A oilfield.

Microfacies	Particle type	Particle content (%)	Pore structure	Sedimentary environment	Log response characteristics
Planktic foraminiferal wackestone	Planktic foraminiferium	25%–50%	Preferably	Deep marine	Low natural gamma, low resistivity, high sonic transit time, low density, and high porosity
Lamellar bioclastic wackestone	Green algae and planktic foraminiferium	50%–80%	Preferably	Back shoal	Low natural gamma values, significantly reduced resistivity compared to adjacent layers, high acoustic transit time, low density, and high neutron porosity
Intraclastic–bioclastic packstone	Biological debris, intraclastic, and a small amount of green algae	40%–55%	Preferably	Bioclastic shoal	Low natural gamma values, significantly reduced resistivity compared to adjacent layers, high acoustic transit time, low density, and high neutron porosity
Green algal packstone	Green algae, Echinodermata, and biological debris	30%–50%	Good pore structure but uneven distribution	Algal mound	High natural gamma values, relatively high resistivity values, high acoustic transit time values, low density, and high porosity
Green alga–pelletoid packstone	Pelletoid, green algae, and a small amount of biological debris	45%–60%	Preferably	Algal mound	Low natural gamma, relatively low resistivity, high acoustic transit time, low density, and high porosity
Bioclastic–intraclastic packstone	Intraclastic, a small amount of biological debris	50%–75%	Medium	Intraclastic shoal	Natural gamma rays have low values, relatively high electrical resistivity, slightly lower acoustic transit time and neutron porosity than adjacent formations, and slightly higher density than adjacent formations
Intraclastic grainstone	Intraclastic, a small amount of green algae, and biological debris	55%–80%	Medium	Intraclastic shoal	Low natural gamma values, high electrical resistivity values, and relatively low three porosity values, with smaller peaks

Two main types of particles exist in MFT2, namely, green algae and planktic foraminiferium, with a small amount of bioclasts. The color of the cores of MFT2 is light brown–gray, with a loose structure and well-developed pores.

The particle types are mainly bioclasts in MFT3, with highest contents of Echinodermata and foraminifera, containing intraclasts and a small amount of green algae. This microfacies contains a high content of matrix, with well-developed pores and areal porosity in the range of 10%–15%.

The particle types are mainly green algae in MFT4, with minor Echinodermata and bioclasts. The green algae are mostly dissolved to form moldic pores. At the same time, the dissolved calcium carbonate precipitates nearby to form cemented patches. Many white dense patches exist that are unevenly distributed on the core. The pores are well developed in this microfacies, with uneven distribution and areal porosity in the range of 15%–21%.

The particle types are mainly intraclasts and green algae in MFT5. Both particle types are unevenly distributed and contain a small amount of bioclasts. Green algae are mostly dissolved to form algal moldic pores. White, dense patches are observed locally on the core. This microfacies has well-developed pores, with a visible porosity of approximately 15%.

The particle type is mainly intraclasts, with a small amount of bioclasts, in MFT6. White, dense patches are observed locally on the core. This microfacies has moderately developed pores, with an areal porosity of less than 7%.

The grain type is mainly intraclastic in MFT7, containing a small amount of green algae and bioclasts, with a very small

amount of marl between the grains. The intraclastic content in this microfacies is greater than 55%, partially or completely cemented by sparry calcite between grains. Unevenly distributed dense patches exist in this microfacies. The microfacies have a moderate development of pores, with an areal porosity of approximately 15%.

4.2 Bioturbation

As the observations in this study were based on plunge cores, there is a lack of macroscopic records and only a few biological burrows (Figure 5A). Lithological zoning due to bioturbation is visible in the thin section, with clear boundaries (Figure 5B). Biological burrows on the surface of calcareous bioclasts are commonly observed (Figures 5C,D).

The Kh2 layer of the A field has mainly developed three species of biological remains, namely, *Thalassinoides*, *Ophiomorpha*, and *Palaeophycus* (Wang Q. et al., 2022; Liu et al., 2019; Shen et al., 2019). *Thalassinoides* remains are developed in all kinds of microfacies. *Thalassinoides* remains are the main bioturbation in the Kh2 layer, resulting in the development of a large number of pores such as intergranular pores. *Thalassinoides*-type remains with a good pore structure are mainly distributed in the green algal debris beach in the middle gentle slope. *Ophiomorpha* remains developed in MFT3, MFT5, and MFT6 microfacies. *Ophiomorpha*-type relics with good pore connectivity are mainly distributed in the medium–low-energy

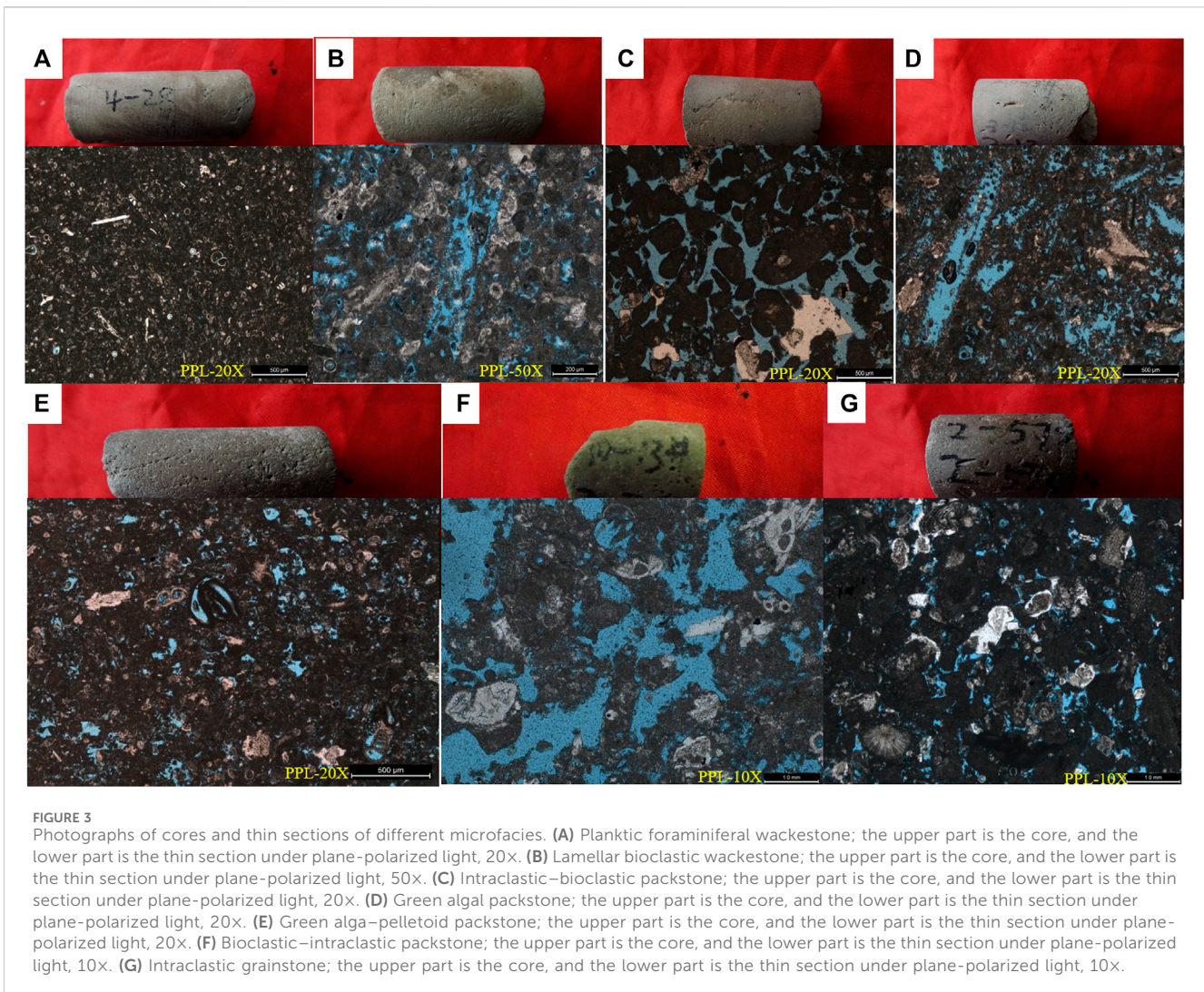


FIGURE 3

Photographs of cores and thin sections of different microfacies. (A) Planktic foraminiferal wackestone; the upper part is the core, and the lower part is the thin section under plane-polarized light, 20x. (B) Lamellar bioclastic wackestone; the upper part is the core, and the lower part is the thin section under plane-polarized light, 50x. (C) Intraclastic-bioclastic packstone; the upper part is the core, and the lower part is the thin section under plane-polarized light, 20x. (D) Green algal packstone; the upper part is the core, and the lower part is the thin section under plane-polarized light, 20x. (E) Green alga-pelletoid packstone; the upper part is the core, and the lower part is the thin section under plane-polarized light, 20x. (F) Bioclastic-intraclastic packstone; the upper part is the core, and the lower part is the thin section under plane-polarized light, 10x. (G) Intraclastic grainstone; the upper part is the core, and the lower part is the thin section under plane-polarized light, 10x.

shoal environment of the moderate slope. *Palaeophycus* remains are found in MFT2, MFT4, and MFT5. *Palaeophycus* remains are mainly distributed in a granular beach environment.

4.3 Diagenesis

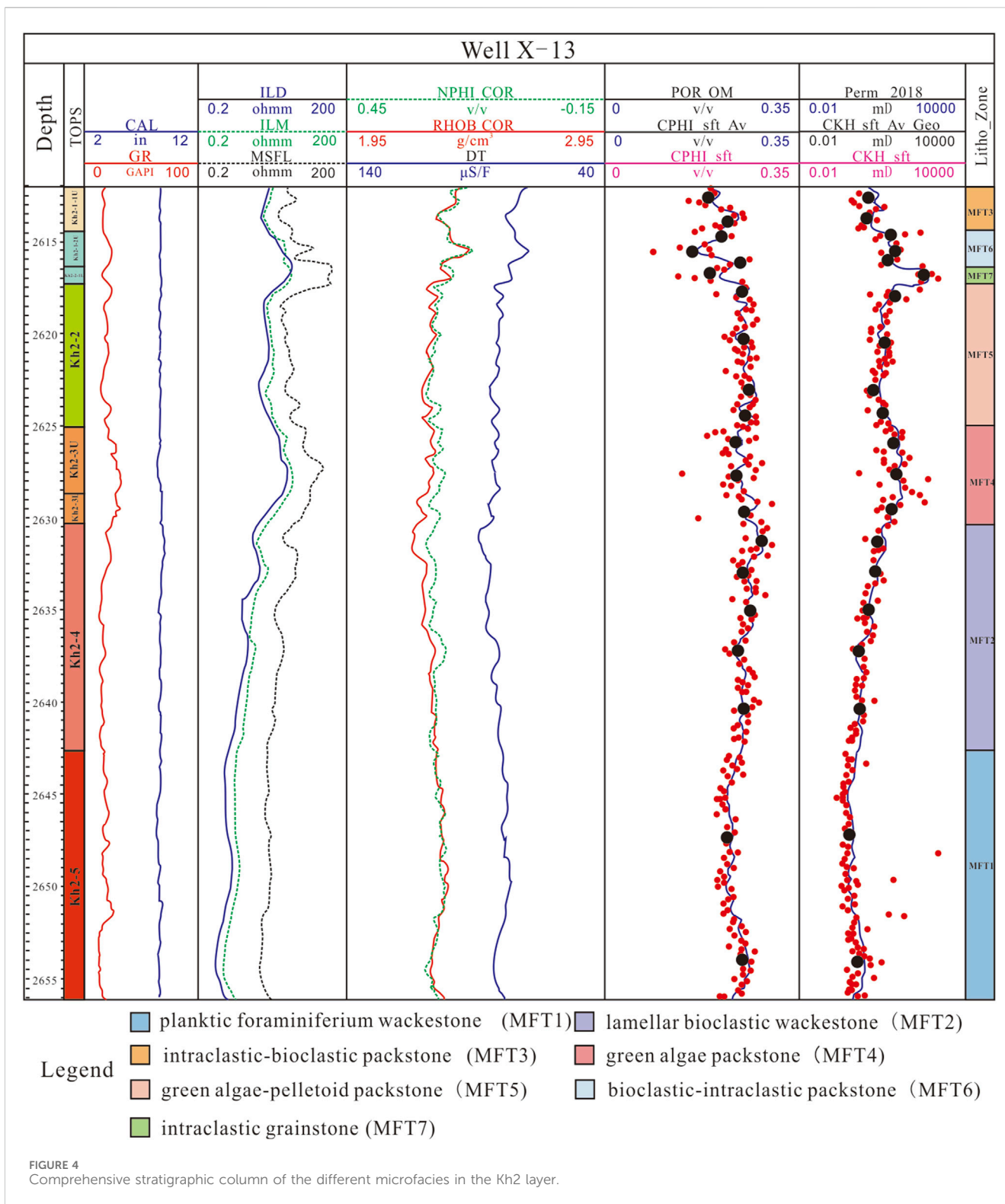
The reservoir quality of the Kh2 layer is mainly controlled by sedimentation and diagenesis. In the study area, bioturbation-superimposed cementation, dissolution, and compaction enhanced the reservoir heterogeneity. By using the contact and position relationship between different diagenetic minerals and the formation time of different dissolution pores, combined with cathodic luminescence, the formation sequence of diagenetic minerals is determined. The formation environment is identified by observing the color of thin sections under cathode luminescence (CL). The color of calcite under CL precipitated from a freshwater environment is usually brighter and that from a seawater environment is dull (Zheng et al., 2020) (Figure 6). The diagenetic sequence of the Kh2 formation in the study area is shown in Figure 7.

4.3.1 Compaction and pressure solution

The results of thin-section identification in the study area show that the granular rock in Kh2 formation is relatively loose. The compaction is weak, and the pressure solution is not strong in the rock, so the effect on the reservoir is small. Most of the particles in the Kh2 formation have point contact, and a small part of them have line contact, which results in increased retention of intergranular pores. The sedimentary fabric of bioclasts in the study area was well-preserved, and no characteristics of dislocation, deformation, and other compaction were observed (Figure 8C). A large number of stylolite can be observed in the cores from the Kh2 layer (Figure 8A).

4.3.2 Cementation

In the Kh2 layer, three types of calcite cements exist, namely, micrite, fiber/needle, and granular calcite. Carbonate rocks were subjected to multi-stage alteration in the diagenetic process to form generational cementation (Figures 8D,E). The first generation often formed in a seawater environment with weak dissolution and developed fibrous/needle calcite rims composed of aragonite. The second and third generations are often formed in



freshwater and burial environments. With the decline in the sea level, the impact of freshwater has increased. With the dissolution of Ca²⁺ in the water combined with CO₃²⁻, isometric granular calcite precipitated by filling dissolved vugs and moldic pores. This phenomenon is widespread in the Khasib Formation in the

study area (Figure 8F) and will deconstruct the quality of the reservoir.

Green algae are mostly dissolved to form moldic pores. At the same time, the dissolved calcium carbonate precipitates nearby to form cemented patches. Many white, dense patches exist near

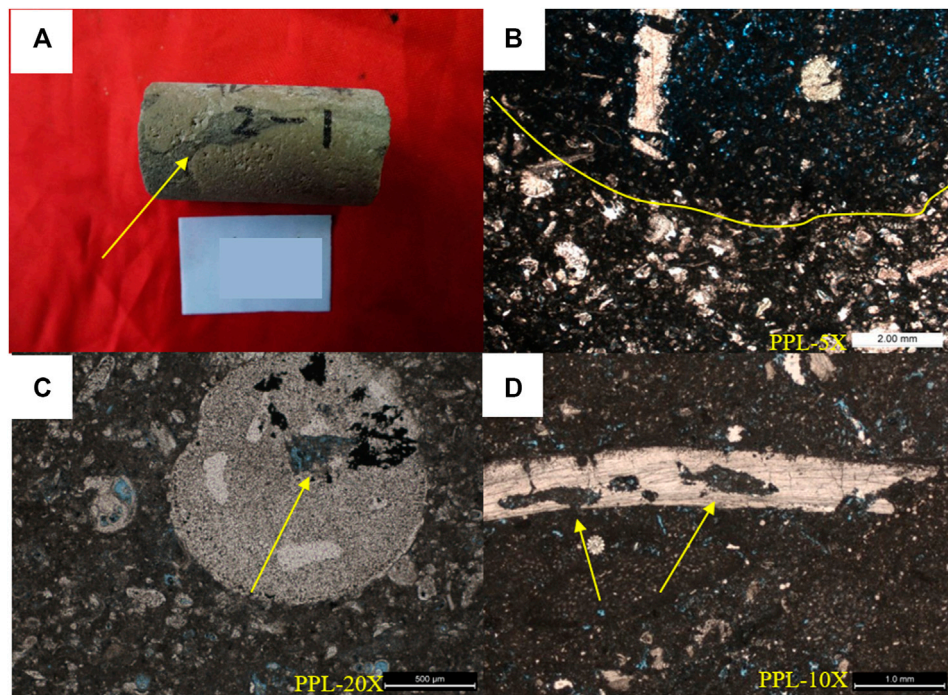


FIGURE 5
Bioturbation evidence from the core and thin sections in the Kh2 layer. (A) Biological burrow, core photograph; (B) boundary of the biological burrow, a thin section under plane-polarized light, 5x; (C) bioturbation on the Echinodermata debris, a thin section under plane-polarized light, 20x; and (D) bioturbation on the bivalve debris, a thin section under plane-polarized light, 10x.

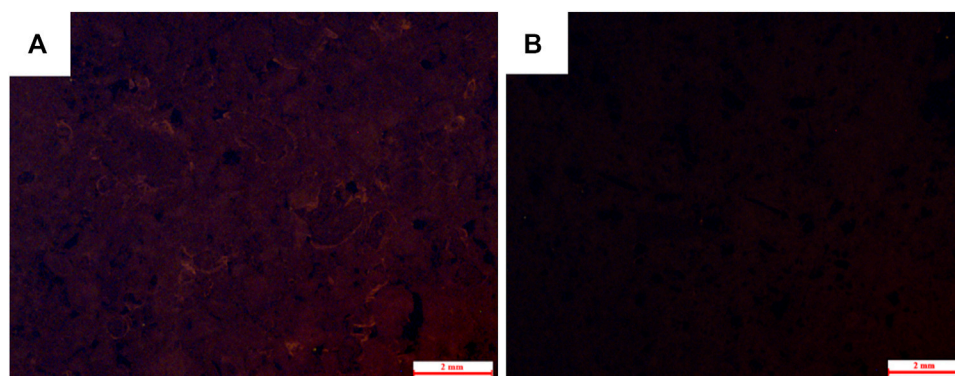


FIGURE 6
Photographs of thin sections under cathode luminescence. (A) Rim of calcite cements with orange–yellow light, the X1-22-1H well, 2756.28 m; (B) micrite with no light, X-6 well, 2689.12 m.

moldic pores. The differential dissolution and cementation induce heterogeneity in this reservoir.

4.3.3 Dissolution

Dissolution is the most important constructive diagenesis of the Khasib Formation in the A oilfield. A large number of secondary pores are formed by the dissolution of the reservoir (Figures 8B,G,H,I). The dissolution of reservoirs in the study area can be roughly divided into four stages. In the first stage, a large number of moldic pores were formed as a result of selective

dissolution of fabrics in the subsurface flow zone of meteoric water. In the second stage, non-fabric, selectively dissolved vugs were formed as a result of the dissolution in the freshwater vadose zone (in this zone, freshwater flows vertically, resulting in strong dissolution). In the third stage, the non-fabric selectively dissolved vugs and fractures were formed as a result of the dissolution in the freshwater vadose zone during the period accompanied by tectonic uplift. In the fourth stage, a small-scale and dense distribution of needle pores formed as a result of burial dissolution. Among the four phases of dissolution, contemporaneous dissolution formed

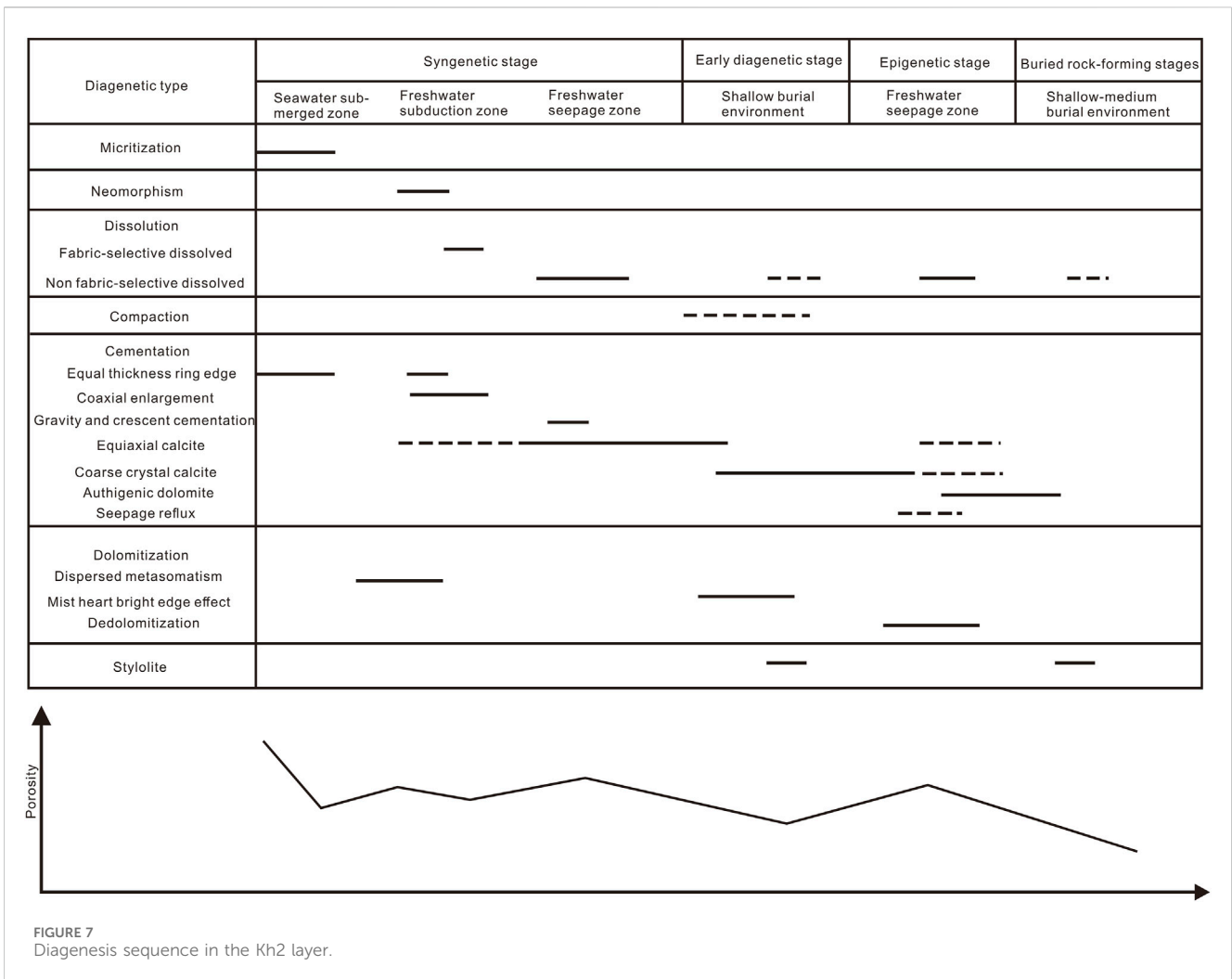


FIGURE 7 Diagenesis sequence in the Kh2 layer.

most of the effective pores in the middle Cretaceous reservoir in the study area.

4.4 Heterogeneity characteristics

4.4.1 Comparison of the heterogeneity of different microfacies

The sublayers in the study area correspond to different microfacies, and statistical evaluation parameters for the heterogeneity of different microfacies are used to characterize the vertical heterogeneity of the reservoir.

In the evaluation of vertical heterogeneity in the study area, the permeability was tested at intervals of 0.125 m. The collected data were categorized into three parameters, namely, variation coefficient, dart coefficient, and range, according to the interval of 1 m, 2 m and 4 m. The statistical results show that the maximum coefficient of variation is 0.99, and the average is about 0.46. The maximum value of the dart coefficient is 5.56, and the average value is about 2.36. The maximum range is 29.26, and the average is about 7.39. As shown in Figure 9, MFT2, MFT6, and MFT7 types have the strongest microfacies heterogeneity. MFT1, MFT3,

MFT4, and MFT5 types have the weakest microfacies heterogeneity.

4.4.2 Comparison of lateral heterogeneity within the same microfacies

Horizontal wells are used to analyze the heterogeneity of different positions in the same layer (same microfacies). Finally, the lateral distribution characteristics of heterogeneity in the same small layer are determined. Because more horizontal well data exist on the Kh2-2, Kh2-3, and Kh2-4 sub-layers in the study area, the lateral heterogeneity of MFT2, MFT4, and MFT5 microfacies is selected for comparative analysis.

In the evaluation of lateral heterogeneity, the permeability was tested at intervals of 0.125 m. The collected data were categorized into three parameters, namely, the variation coefficient, dart coefficient, and range, according to the interval of 10 m, 20 m, and 40 m, respectively. The statistical results show that the maximum coefficient of variation is 0.99, and the average is about 0.46. The maximum value of the dart coefficient is 5.56, and the average value is about 2.36. The maximum range is 29.26, and the average is about 7.39. Figure 10 shows that the MFT2 type has the strongest lateral heterogeneity, while MFT4 and

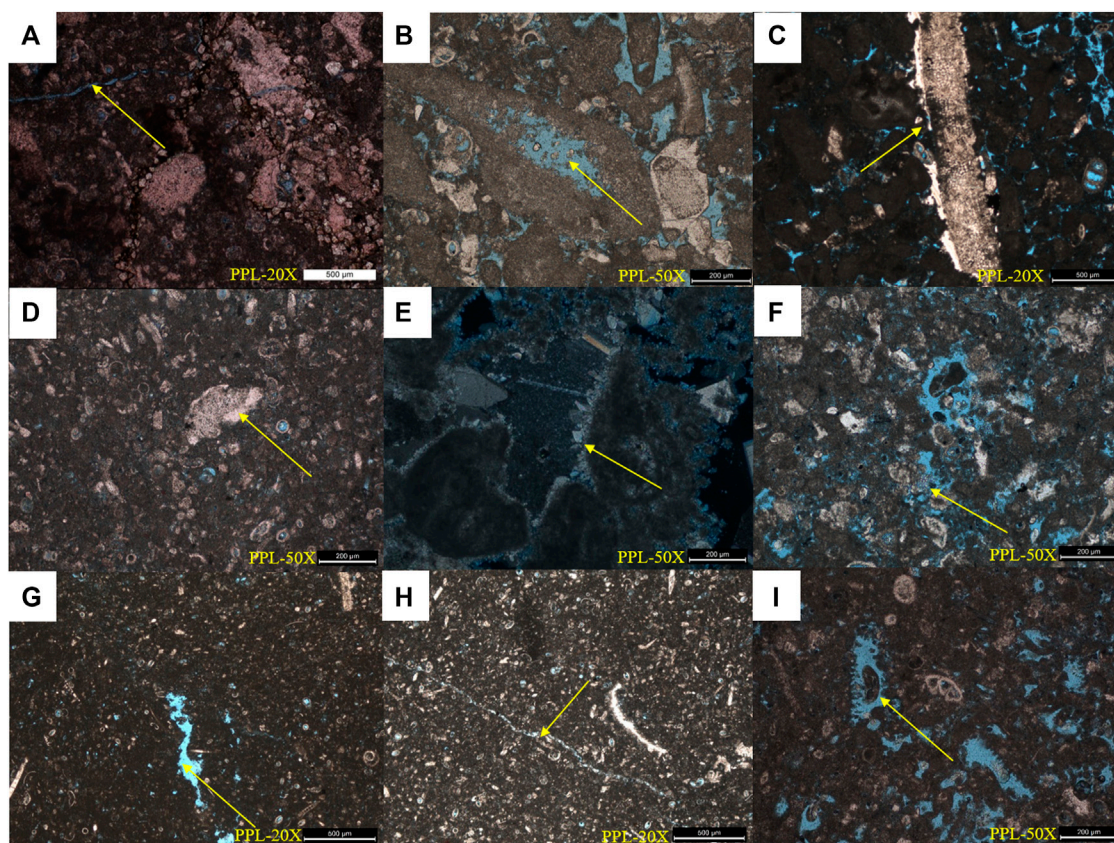


FIGURE 8 Photographs of diagenetic alteration in the Kh2 layer. (A) Pressure solution, X-12 well, 2817.88 m, visible stylolite, a thin section under plane-polarized light, 20x. (B) Dissolution, X-13 well, 2616 m, a thin section under plane-polarized light, 50x. (C) Pressure dissolution of the edge of the Echinodermata, X-13 well, 2614 m, a thin section under plane-polarized light, 20x. (D) Echinodermata coaxial overgrowth, X-13 well, 2634 m, a thin section under plane-polarized light, 50x. (E) Calcite generation cementation, X-13 well, 2953.77 m, a thin section under plane-polarized light, 50x. (F) Granular calcite filling, X-13 well, 2630 m, a thin section under plane-polarized light, 50x. (G) Non-fabric selective dissolution, X-13 well, 2641 m, a thin section under plane-polarized light, 20x. (H) Fracture, X-13 well, 2638 m, a thin section under plane-polarized light, 20x. (I) Algal moldic pore, X-13 well, 2637 m, a thin section under plane-polarized light, 50x.

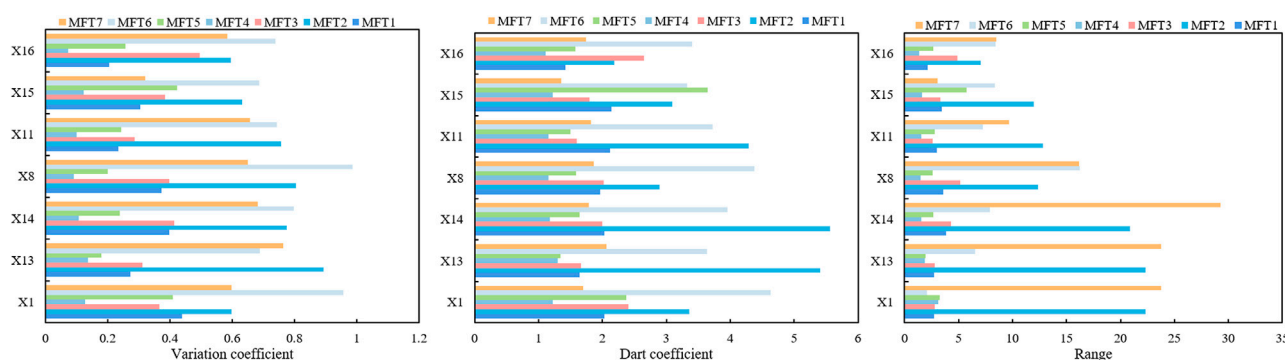
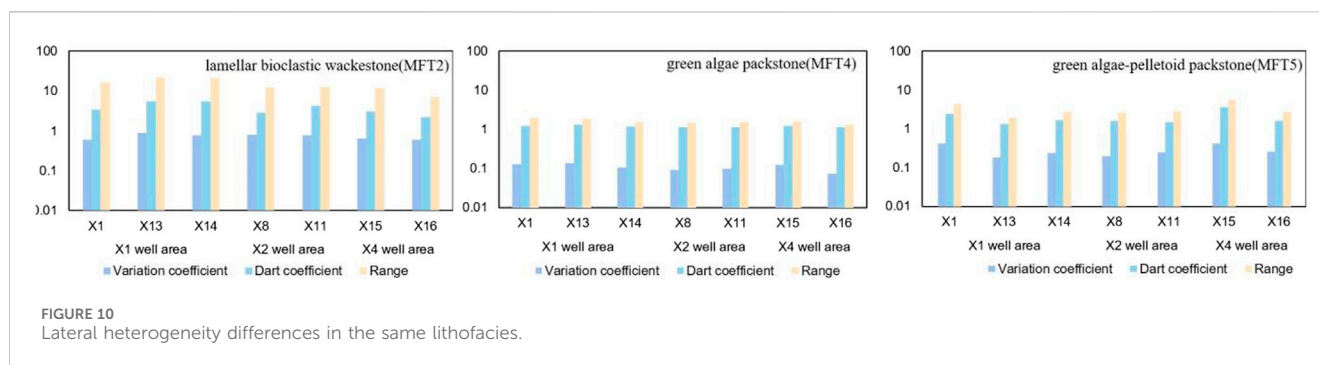


FIGURE 9 Differences in the vertical heterogeneity of different microfacies.

MFT5 types have weaker lateral heterogeneity. The results are consistent with the vertical heterogeneity trend discussed in the previous section. Differences in reservoir heterogeneity also exist

between different well zones. On the whole, there is a gradual weakening trend of vertical and lateral heterogeneity from well areas X1–X4.



5 Discussion

By calculating the variation coefficient of the reservoir in the study area, the heterogeneity between different microfacies can be compared. The microfacies with strong heterogeneity are MFT2, MFT6, and MFT7. Table 1 in Section 3.1 shows that the particle content of the three microfacies is the highest among the seven microfacies. The effects of particle types, bioturbation characteristics, content and distribution of green algae, and differences in dissolution and cementation of the three microfacies were analyzed. The heterogeneous pattern of the Kh2 layer is established.

5.1 Particle type controls on the heterogeneity of bioclastic limestone

The carbonate rocks of the Khasib Formation in the study area are composed of marl and various types of skeleton fragments, with a small amount of non-skeleton fragments. The skeleton debris includes foraminifera, green algae, bivalve, Echinodermata, and rudist. Non-skeletal particles contain pelletoids and intraclasts. The impact of particles on reservoir heterogeneity is mainly reflected in the relative content of bioclastic and intraclast.

The relative contents of algae, other bioclasts, and intraclasts of the three types of microfacies were calculated, and their coefficients of variation were calculated (Table 2). It can be concluded that the microfacies with a high particle content has strong heterogeneity. However, the influence of bioclastic content on heterogeneity is greater than that of the intraclast content. Moreover, the facies with a high algal content are more heterogeneous. Because the green algae in the study area are mainly aragonite mineral, they are easy to dissolve and produce a large number of algal moldic pores, resulting in a strong heterogeneity of the reservoir.

The distribution pattern and content of green algae in different microfacies are different. By studying the difference of distribution patterns of green algae in study areas, the influence of different distribution patterns on reservoir heterogeneity was clarified. The distribution patterns of green algae in the study area were divided into three types: aggregated, dispersed, and isolated (Figure 11). The high content of green algae in the

aggregate type and the dissolution of connectivity are conducive to the improvement of reservoir permeability, resulting in the enhancement of reservoir heterogeneity. The content of green algae is high but dispersed. After dissolution, the permeability of the reservoir does not increase significantly, and the distributed distribution mode slightly enhances the heterogeneity of the reservoir. The isolated pattern has little effect on reservoir heterogeneity due to the low content of green algae. It can be proved by calculating the coefficient of variation of the above three patterns (Figure 11).

5.2 Bioturbation influences on the heterogeneity of MT2

Among the three types of microfacies discussed in Section 4.1, MFT2 has the strongest heterogeneity and the highest content of bioclastics. Analysis of thin-section photographs and core photographs at different depths in MFT2 microfacies (Table 3) showed obvious different lithologies in the same thin section under the microscope, and obvious bioturbation can be seen on the core, with a high coefficient of variation and strong heterogeneity, in areas with strong biological disturbance. Therefore, it is believed that there is a positive correlation between the intensity of biological disturbance and the intensity of reservoir heterogeneity.

5.3 Differential dissolution and cementation can change the heterogeneity of the bioclastic limestone reservoir

Dissolution can occur at various diagenetic stages of carbonate rocks, and a large number of secondary pores can be formed. The dissolution mechanism of carbonate rocks can be divided into near-surface freshwater dissolution, organic acid dissolution in a burial environment, hydrothermal dissolution, etc. (Zhang et al., 2021). Cementation is one of the key deconstruction factors in carbonate diagenesis. As a result of cementation, crystal growth occurs in the intergranular pores, and the reservoir is damaged. The carbonate cements mainly consist of the fibrous crystal and coarse-grained crystal (Gong and Jiang, 2009). Dissolution and cementation are usually

TABLE 2 Statistical result for the proportion of particle content in different microfacies.

Microfacies type	Particle content (%)			
	Other biological debris (%)	Intraclastic grain (%)	Algae (%)	Coefficient of variation
Lamellar bioclastic wackestone (MFT2)	68	22	10	0.60–0.90
Bioclastic–intraclastic packstone (MFT6)	25	70	5	0.68–0.96
Intraclastic grainstone (MFT7)	8	90	2	0.32–0.66

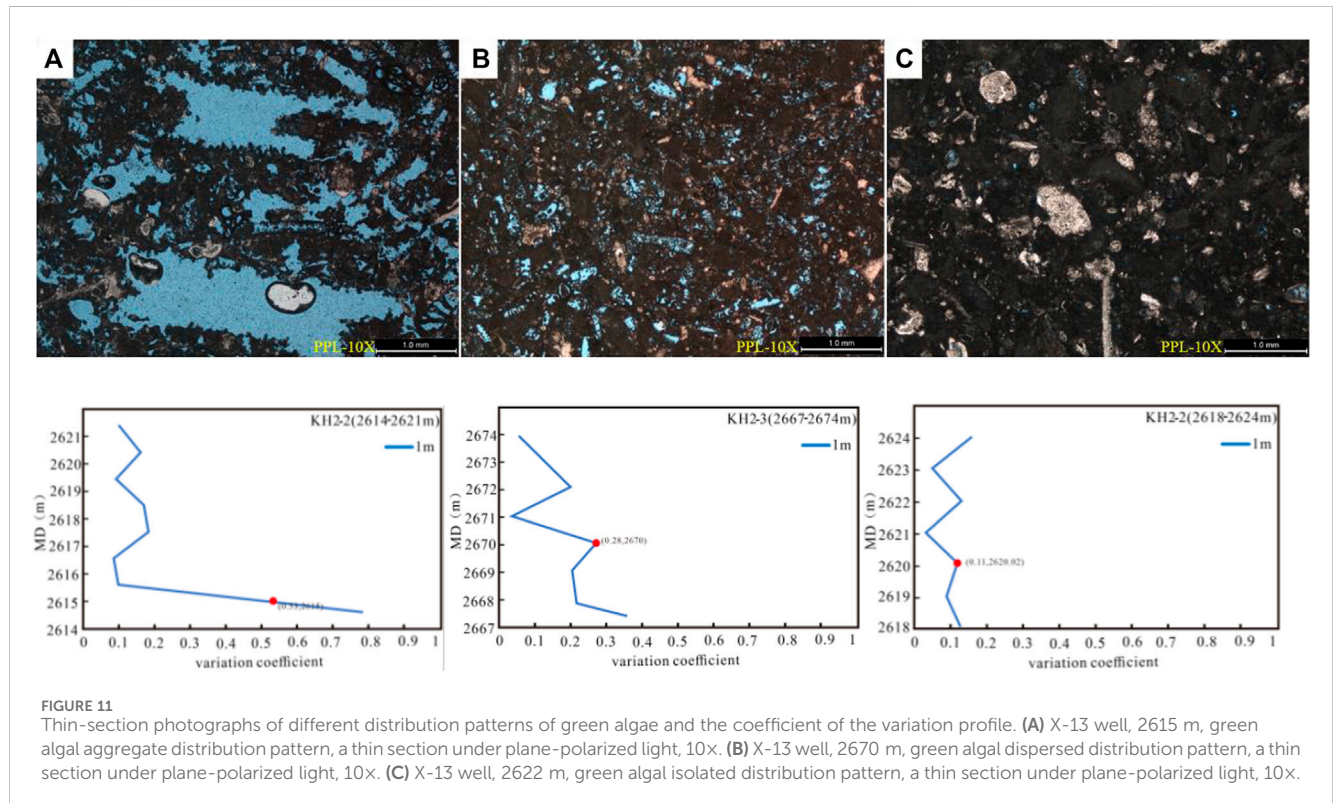


FIGURE 11 Thin-section photographs of different distribution patterns of green algae and the coefficient of the variation profile. (A) X-13 well, 2615 m, green algal aggregate distribution pattern, a thin section under plane-polarized light, 10x. (B) X-13 well, 2670 m, green algal dispersed distribution pattern, a thin section under plane-polarized light, 10x. (C) X-13 well, 2622 m, green algal isolated distribution pattern, a thin section under plane-polarized light, 10x.

TABLE 3 Relationship between biological disturbance and heterogeneity.

Well location	Zone	Depth(m)	Biological disturbance intensity	Thin-film photograph	Core photograph	Coefficient of variation	Heterogeneity
X-13 well	Kh2-4	2607.81	Strong			0.67	Strong
		2605.03	Medium			0.35	Medium
		2609.67	Weak			0.13	Weak

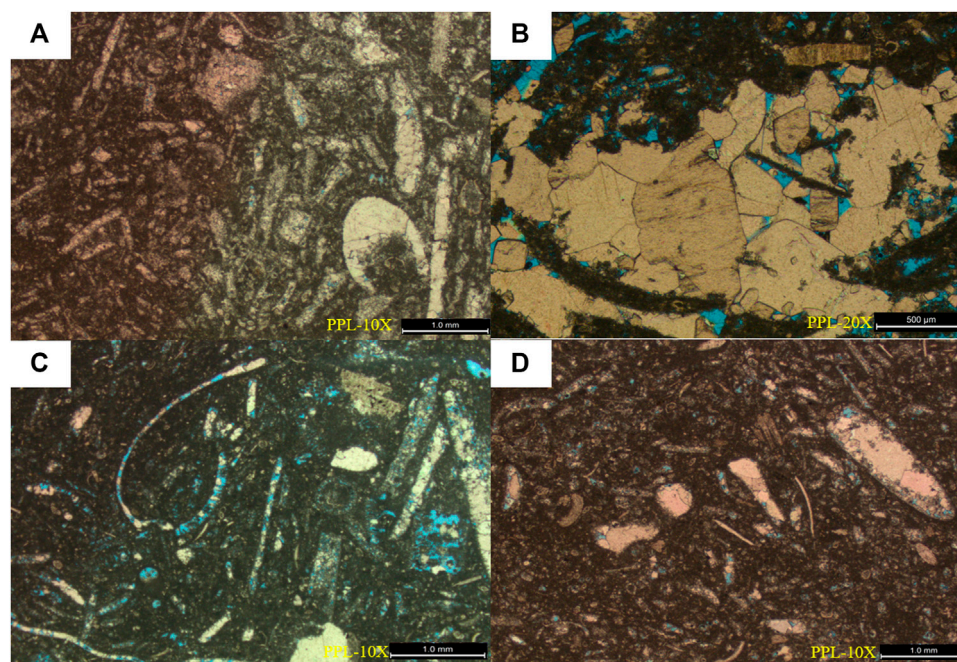


FIGURE 12
 Characteristics of rock subjected to cementation (the pores formed during the dissolution process are filled by the precipitation of dissolution products). (A) XMa-4H-2770.62 m, a thin section under plane-polarized light, 10x. (B) XMa-4H-2770.17 m, a thin section under plane-polarized light, 20x. (C) XMa-4H-2777.73 m, a thin section under plane-polarized light, 10x. (D) XMa-4H-2784.04 m, a thin section under plane-polarized light, 10x.

associated with each other, and both affect the reservoir heterogeneity.

The carbonate sediments in the study area were mainly green algae and Echinodermata. The green algae were dissolved to form algal moldic pores, and calcium carbonate was dissolved and precipitated to form cemented patches. Dissolution will further expand the pores, and cementation will reduce the pore space. According to the research in Section 4.1, the distribution of green algae in the study area is uneven. Therefore, non-fabric selective dissolution, selective dissolution, and differential cementation exist in the study area. These three diageneses will lead to uneven pore development and further enhance the heterogeneity of the study area. For example, the cementation degree of the X-Ma4H well in the working area is strong. It can be observed that the moldic pores and the dissolved pores are completely filled with calcite (Figure 12). Although the pores developed in these microfacies, the distribution of pores is not uniform, and the heterogeneity is strong.

5.4 Heterogeneity pattern in the study area

According to the above discussion, the heterogeneity of the study area is mainly controlled by the content and type of particles, the distribution pattern of green algae, bioturbation, and differential dissolution and cementation. Based on the above factors, a geological pattern of reservoir heterogeneous development was established in the study area (Figure 13).

In the study, grainstone, packstone, and wackestone are deposited on the carbonate ramp in the Khasib Formation. Some

similar cases including the Lower-Cretaceous Yamama Formation in the southeastern part of the basin (Fadhil, 1993); the Middle-Cretaceous Sarvak Formation in the Zagros Basin, southwestern Iran (Mohammad et al., 2016; Elham et al., 2013); the Upper-Cretaceous Shiranish Formation; and the internal reservoirs of the Middle-Cretaceous Maaddud Formation in the Arabian Gulf Basin are all similar (Sadooni, 2004; El-Anbaawy and sadek, 1979). Therefore, the development pattern of reservoir heterogeneity studied in this paper is universal.

6 Application

The A oilfield is a highly heterogeneous carbonate reservoir, so it is necessary to understand the oil-water relationship in waterflood development. Tracer interwell monitoring techniques are often used for research (Cheng, 2005). A tracer is a chemical agent that can flow with a fluid and indicate the presence, direction, and speed of movement of the fluid. The application of a tracer for interwell monitoring means that the water-soluble tracer is injected into the injection well, and water samples are taken from the surrounding monitoring wells. According to the time and concentration of the tracer in the water samples, the interpretation results obtained can not only reflect the longitudinal connectivity between wells but also the distribution of the remaining oil (Ding et al., 2007). In this paper, by selecting well X1-13-X in the strong-heterogeneity area and wells X1-13-Y and X1-13-Z in the weak-heterogeneity area for the tracer test (Table 4), it is concluded that the strength of heterogeneity has a good corresponding relationship with the presence of the tracer. In

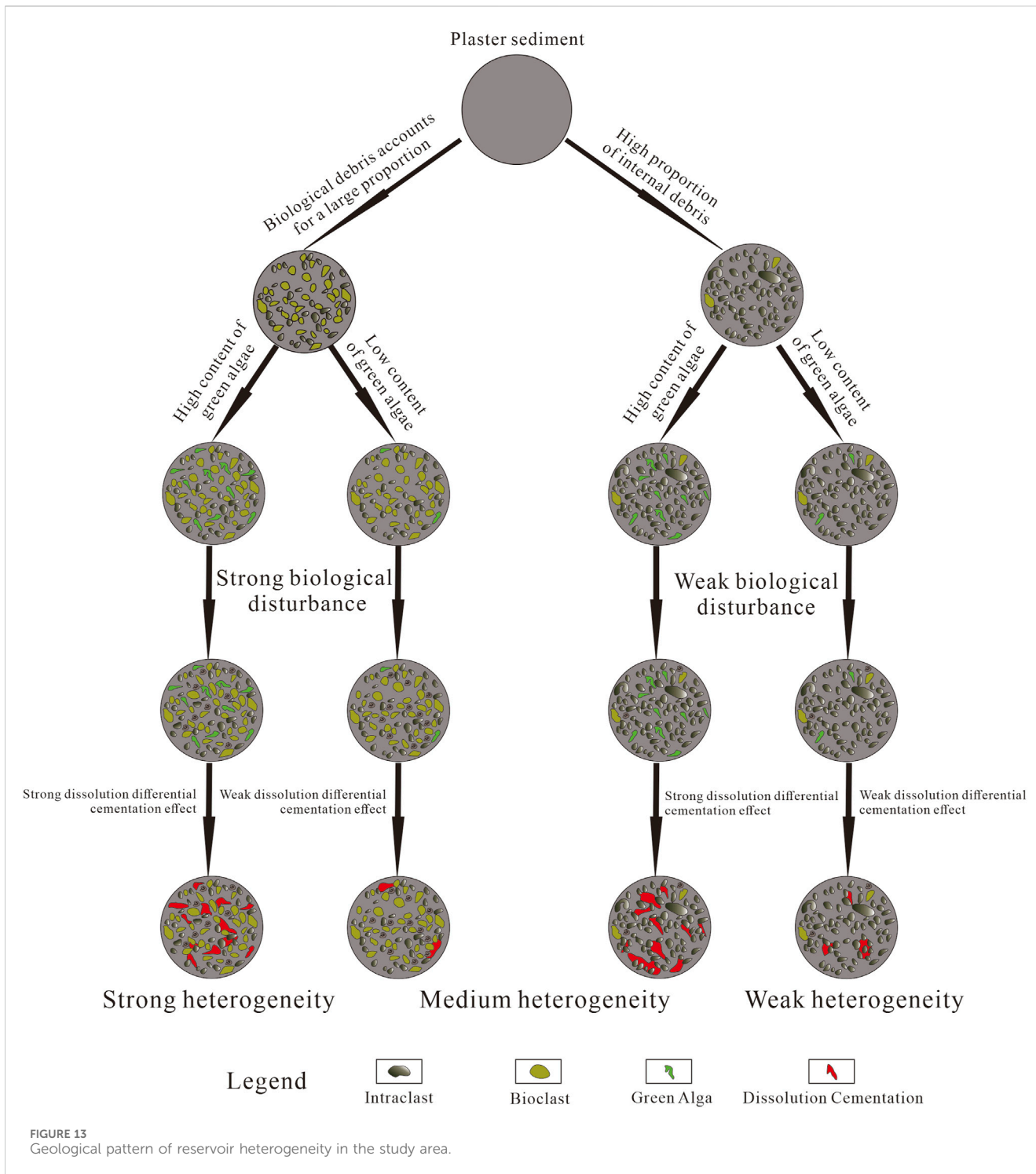


TABLE 4 Tracer test well.

Well	Well spacing(m)			Tracer appearance time Day	Advance speed				Tracer proportion Accumulate (%)
	Near	Middle	Far		Near	Middle	Far	Average	
X1-13-X	300	600	900	96	3.1	6.3	9.4	6.3	7
X1-13-Y	300	600	900	29	10.3	10.3	10.3	10.3	37
X1-13-Z	300	600	900	47	6.4	12.8	19.1	12.8	9

the strong-heterogeneity area, the water content increases slowly in terms of the presence time of the tracer. In the weak-heterogeneity area, the time of the application of the well-location tracer is short, and the water cut increases rapidly.

7 Conclusion

- (1) Seven types of microfacies developed in the Kh2, namely, planktic foraminiferal wackestone (MFT1), lamellar bioclastic wackestone (MFT2), intraclastic–bioclastic packstone (MFT3), green algal packstone (MFT4), green alga–pelletoid packstone (MFT5), bioclastic–intraclastic packstone (MFT6), and intraclastic grainstone (MFT7). The calculation of the three parameters, coefficient of variation, dart coefficient, range and statistics, showed that the heterogeneity of striated bioclastic wackestone (MFT2) is the strongest.
- (2) Comprehensive analysis shows that the reservoir heterogeneity in the study area is mainly affected by the content and type of particle. The higher the particle content, the stronger the heterogeneity. The influence of the content and type of bioclastic on the heterogeneity is greater than that of intraclast.
- (3) The distribution patterns of green algae in the study area were divided into three types: aggregated, dispersed, and isolated patterns. In the distribution pattern of green algae, the reservoir heterogeneity is strongest in the aggregated distribution pattern.
- (4) The stronger the bioturbation, the stronger the heterogeneity. The degree of dissolution–cementation is different in different microfacies, and the microfacies with a high degree of dissolution–cementation are more heterogeneous.

Data availability statement

The raw data supporting the conclusion of this article will be made available by the authors, without undue reservation.

Author contributions

CL: data curation, writing–original draft, and writing–review and editing. XZ: conceptualization, formal analysis, visualization,

writing–original draft, and writing–review and editing. MF: conceptualization, formal analysis, methodology, and writing–review and editing. TH: methodology, supervision, validation, and writing–review and editing. GD: investigation and writing–review and editing. SG: investigation and writing–review and editing.

Funding

The author(s) declare that no financial support was received for the research, authorship, and/or publication of this article.

Acknowledgments

The author expresses their gratitude to all those who helped them during the writing of this manuscript. The author thanks the State Key Laboratory of Oil and Gas Reservoir Geology and Exploitation (Chengdu University of Technology) for their assistance in the experimental research involved in this paper. The author also thanks Petrochina Chuanqing Drilling Engineering Co., Ltd., for providing the experimental samples needed for this study.

Conflict of interest

Author TH was employed by China Petroleum Formation Chuanqing Drilling Engineering Co., Ltd.

The remaining authors declare that the research was conducted in the absence of any commercial or financial relationships that could be construed as a potential conflict of interest.

Publisher's note

All claims expressed in this article are solely those of the authors and do not necessarily represent those of their affiliated organizations, or those of the publisher, the editors, and the reviewers. Any product that may be evaluated in this article, or claim that may be made by its manufacturer, is not guaranteed or endorsed by the publisher.

References

- Abdel-Fattah, M. I., Mahdi, A. Q., Theyab, M. A., Pigott, J. D., Abd-Allah, Z. M., and Radwan, A. E. (2022). Lithofacies classification and sequence stratigraphic description as a guide for the prediction and distribution of carbonate reservoir quality: a case study of the Upper Cretaceous Khasib Formation (East Baghdad oilfield, central Iraq). *J. Petroleum Sci. Eng.* 209, 109835. doi:10.1016/j.petrol.2021.109835
- Al-Qayim, B. (2010). Sequence stratigraphy and reservoir characteristics of the turonian-coniacian khasib formation in central Iraq. *J. Petroleum Geol.* 33 (4), 387–403. doi:10.1111/j.1747-5457.2010.00486.x
- Alsuwaidi, M. E., Mohamed, A. A. I., Mansurbeg, H., Morad, S., Alsuwaidi, A., Al-Shalabi, E. W., et al. (2021). Depositional and diagenetic controls on reservoir quality of microporous basinal lime mudstones (Aptian), United Arab Emirates. *Sediment. Geol.* 420, 105925. doi:10.1016/j.sedgeo.2021.105925
- Aqrabi, A. A. M. (1997). The nature and preservation of organic matter in holocene lacustrine/deltaic sediments of lower mesopotamia, se Iraq. *J. Petroleum Geol.* 20 (1), 69–90. doi:10.1306/bf9ab77f-0eb6-11d7-8643000102c1865d
- Chen, H. Q., Wang, Y., and Du, Y. J. (2017). Advances of research methods on reservoir heterogeneity. *Geol. J. China Univ.* (01), 104–116. doi:10.16108/j.issn1006-7493.2016060
- Chen, M. J., Cheng, L., and Lu, T. (2020). Pore structure characterization and its impact on waterflooding development in Khasib reservoir in Ahdeb Oilfield, Iraq. *Lithol. Reserv.* (03), 133–143. doi:10.12108/xyqc.20200313
- Chen, S. Y. (2005). The method of interwell tracer and heterogeneity of reservoir. *Ind. Mong. Petrochem. Ind.* (09), 76–79. doi:10.3969/j.issn.1006-7981.2005.09.041
- Dunham, R. J. (1962). "Classification of Carbonate rocks according to depositional texture, 108–121. AAPG Memoir 1.
- El-Anbaawy, M. I. H., and Sadek, A. (1979). Paleocology of the shirani formation (maastrichtian) in northern Iraq by means of microfacies analysis and clay mineral investigation. *Palaeogeogr. Palaeoclimatol. Palaeoecol.* 26, 173–180. doi:10.1016/0031-0182(79)90148-2

- Elfeki, A., and Dekking, M. (2001) Markov chain model for subsurface characterization: theory and applications. DIOC Symposium 0.
- Elham, A. M., Mohammad, H. A., and Adam, D. W. (2013). Microfacies and geochemistry of the middle cretaceous Sarvak Formation in Zagros Basin, izeh zone, SW Iran. *Sediment. Geol.* 293, 9–20. doi:10.1016/j.sedgeo.2013.04.005
- Fadhil, N. S. (1993). Stratigraphic sequence, microfacies, and petroleum prospects of the Yamama Formation, Lower Cretaceous, southern Iraq. *Geosci. World* 77 (11). doi:10.1306/bdff8f92-1718-11d7-8645000102c1865d
- Farouk, S., Al-Kahtany, K., and Abdelhady, A. A. (2022). Cyclic nature of the biotic attributes of macroinvertebrate communities in the Cenomanian–Turonian strata of Sinai: water depth-driven biological responses. *Facies* 68 (1), 1–25. doi:10.1007/s10347-021-00639-8
- Gingras, M. K., Pemberton, S. G., and Smith, M. (2014). Bioturbation: reworking sediments for better or worse. *Oilfield Rev.* 46 (6), 46–58.
- Gong, Y. C., and Jiang, R. (2009). Influence of carbonate diagenesis on carbonate reservoir A case study from cementation. *Inn. Mong. Petrochem. Ind.* (24), 174–176.
- Guo, R., Fu, M. Y., Zhao, L. M., Duan, T. X., Han, H. Y., Huang, T. T., et al. (2014). Sediment facies of khabib formation in ahdeb oil field and its controlling effects on carbonate reservoir development. *J. Mineralogy Petrology* (01), 95–103. doi:10.19719/j.cnki.1001-6872.2014.01.014
- Han, H. Y., Mu, L. X., Guo, R., Zhao, L. M., and Su, H. Y. (2014). Characteristics and controlling factors of cretaceous bioclastic limestone reservoirs in ahdeb oil field, Iraq. *Mar. Orig. Pet. Geol.* (02), 54–63. doi:10.3969/j.issn.1672-9854.2014.02.008
- Haq, B. U., and Al-Qahtani, A. M. (2005). Phanerozoic cycles of sea-level change on the arabian platform. *GeoArabia. Middle East Pet. Gepscoence* 10 (2), 127–160. doi:10.2113/geoarabia1002127
- Jodeyri-Agahi, R., Rahimpour-Bonab, H., Tavakoli, V., Kadkhodaie-Ilkhchi, R., and Yousefpour, M.-R. (2018). Integrated approach for zonation of a mid-cenomanian carbonate reservoir in a sequence stratigraphic framework. *Geol. Acta* (3), 321–337. doi:10.1344/GeologicaActa2018.16.3.5
- Khazaie, E., Noorian, Y., Kavianpour, M., Moussavi-Harami, R., Mahboubi, A., and Omidpour, A. (2022). Sedimentological and diagenetic impacts on porosity systems and reservoir heterogeneities of the Oligo-Miocene mixed siliciclastic and carbonate Asmari reservoir in the Mansuri oilfield, SW Iran. *J. Petroleum Sci. Eng.* 213, 110435. doi:10.1016/j.petro.2022.110435
- Li, F. F., Li, L., and Yu, Y. C. (2023). Reservoir intense heterogeneity and main controlling factors of thick bioclastic limestone in X Oilfield, Iraq. *J. Northeast Petroleum Univ.* (01), 84–95. doi:10.3969/j.issn.2095-4107.2023.01.007
- Liu, H. Y., Shi, K. B., Liu, B., Song, X. M., Guo, R., Li, Y., et al. (2019). Characterization and identification of bioturbation-associated high permeability zones in carbonate reservoirs of Upper Cretaceous Khasib Formation, AD oilfield, central Mesopotamian Basin, Iraq. *Mar. Petroleum Geol.* 110, 747–767. doi:10.1016/j.marpetgeo.2019.07.049
- Liu, H. Y., Shi, K. B., Liu, B., Song, X. M., Guo, R., Wang, G. J., et al. (2021). Microfacies and reservoir quality of the middle cretaceous rumaila Formation in the AD oilfield, central Mesopotamian Basin, southern Iraq. *J. Asian Earth Sci.* 213, 104726. doi:10.1016/j.jseaes.2021.104726
- Mahdi, T. A., and Aqrabi, A. A. M. (2014). Sequence stratigraphic analysis of the mid-cretaceous mishrif formation, southern mesopotamian basin, Iraq. *J. Petroleum Geol.* 37 (3), 287–312. doi:10.1111/jpg.12584
- Mao, X. Y., Song, B. B., Han, R. B., Tian, C. B., Li, B. Z., and Song, H. Q. (2020). Depositional characteristics of tidal channel facies in carbonate ramp of the Cretaceous Mishrif Formation in southern Iraq (Article). *Oil Gas Geol.* (06), 1233–1256. doi:10.11743/ogg20200611
- Mirzaei, M., and Das, D. B. (2007). Dynamic effects in capillary pressure-saturations relationships for two-phase flow in 3d porous media: implications of micro-heterogeneities. *Chem. Eng. Sci.* 62 (7), 1927–1947. doi:10.1016/j.ces.2006.12.039
- Mohammad, H., Adabi, U. K., and Abbas, S. (2016). Sedimentary facies, depositional environment, and sequence stratigraphy of Oligocene–Miocene shallow water carbonate from the Rig Mountain, Zagros basin (SW Iran). *Carbonates Evaporites* 31 (1), 69–85. doi:10.1007/s13146-015-0242-9
- Mohammed, A., Dhaidan, M., Al-Hazaa, S. H., and Al-Kahtany, K. (2022). Reservoir characterization of the upper Turonian – lower Coniacian Khasib formation, South Iraq: implications from electrofacies analysis and a sequence stratigraphic framework. *J. Afr. Earth Sci.* 186, 104431. doi:10.1016/j.jafrearsci.2021.104431
- Mohammed, I. Q., Farouk, S., and Mousa, A. (2022). Lithofacies types, mineralogical assemblages and depositional model of the Maastrichtian–Danian successions in the Western Desert of Iraq and eastern Jordan. *J. Afr. Earth Sci.* 186.
- Mohsin, M., Tavakoli, V., and Jamalain, A. (2023). The effects of heterogeneity on pressure derived porosity changes in carbonate reservoirs, Mishrif formation in SE Iraq. *Petroleum Sci. Technol.* 41 (8), 898–915. doi:10.1080/10916466.2022.2070210
- Nazemi, M., Tavakoli, V., Rahimpour-Bonab, H., and Sharif-Yazdi, M. (2021). Integrating petrophysical attributes with saturation data in a geological framework, Permian–Triassic reservoirs of the central Persian Gulf. *J. Afr. Earth Sci.* 179, 104203. doi:10.1016/j.jafrearsci.2021.104203
- Radwan, A. E., Nabawy, B. S., and Kassem, A. A. (2021). Implementation of rock typing on waterflooding process during secondary recovery in oil reservoirs: a case study, El morgan oil field, Gulf of suez, Egypt. *Nat. Resour. Res.* 452. doi:10.1007/s11053-020-09806-0
- Sadooni, F. N. (2004). Stratigraphy, depositional setting and reservoir characteristics of turonian - campanian carbonates in central Iraq. *J. Petroleum Geol.* 27 (4), 357–371. doi:10.1111/j.1747-5457.2004.tb00063.x
- Sadooni, F. N., and Alsharhan, A. S. (2003). Stratigraphy, microfacies, and petroleum potential of the Maaddud Formation (Albian–Cenomanian) in the arabian Gulf Basin. *AAPG Bull.* 87 (10), 1653–1680. doi:10.1306/04220301111
- Shao, X. J. (2010). A new parameter for characterizing heterogeneity of reservoir permeability - calculation method and significance of permeability stagnation coefficient. *Petroleum Geol. Exp.* (04), 397–399+404. doi:10.11781/sydz201004397
- Sharif-Yazdi, M., Rahimpour-Bonab, H., Nazemi, M., Tavakoli, V., and Gharechelou, S. (2020). Diagenetic impacts on hydraulic flow unit properties: insight from the Jurassic carbonate Upper Arab Formation in the Persian Gulf. *J. Petroleum Explor. Prod. Technol.* 10 (5), 1783–1802. doi:10.1007/s13202-020-00884-7
- Shen, Y. C., Song, X. M., Liu, B., Wang, G. J., Guo, R., Luo, Q. Q., et al. (2019). Bioturbation and reservoir heterogeneity study of upper cretaceous Kh2 member, AD oilfield, Iraq. *Nat. Gas. Geosci.* (12), 1755–1770. doi:10.11764/j.issn.1672-1926.2019.07.017
- Sherwani, G. H. M., and Aqrabi, A. A. M. (1987). Lithostratigraphy and environmental considerations of cenomanian-early turonian shelf carbonates (rumaila and mishrif formations) of mesopotamian basin, middle and southern Iraq. *Aapg Bull.*
- Tavakoli, V., Hassani, D., Rahimpour-Bonab, H., and Mondak, A. (2022). How petrophysical heterogeneity controls the saturation calculations in carbonates, the Barremian–Aptian of the central Persian Gulf. *J. Petroleum Sci. Eng.* 208, 109568. doi:10.1016/j.petro.2021.109568
- Tian, Z. Y., Guo, r., and Yu, G. Y. (2020). Characters and petrophysical evaluations of different super-permeability zones in the cretaceous bioclastic limestone reservoirs – a case study of AA field, Iraq[J]. *Springer Series in Geomechanics and Geoenvironmenting*, 1995–2007. doi:10.1007/978-981-15-2485-1_180
- Wang, G. J., Song, X. M., Liu, B., and Shi, K. B. (2022). Effect of bioturbation on reservoir heterogeneity of the upper cretaceous khasib Formation in AD oilfield, Iraq. *Mar. Orig. Pet. Geol.* (01), 11–20. doi:10.3969/j.issn.1672-9854.2022.01.002
- Wang, L. E., and Jiang, F. D. (2009). Quantitative characterization method for heterogeneity of carbonate reservoirs. *Nat. Gas. Technol.* (01), 27–29+78. doi:10.11764/j.issn.1672-1926.2017.11.002
- Wang, Q., Wen, T., Li, H. X., Zeng, X. Y., Wang, X. Z., Xin, J., et al. (2022). Influence of heterogeneity on fluid property variations in carbonate reservoirs with multistage hydrocarbon accumulation: a case study of the Khasib formation, Cretaceous, AB oilfield, southern Iraq. *Open Geosci.* 14 (1), 663–674. doi:10.1515/GEO-2022-0363
- Wang, X. X., Hou, J. G., and Liu, Y. M. (2017). Quantitative characterization of heterogeneity in estuary dams based on analytic hierarchy process and fuzzy mathematics: a case study of Guan195 fault block in wangguantun oilfield. *Nat. Gas. Geosci.* (12), 1914–1924.
- Xu, H. (2018). *A study on the characteristics of carbonate reservoir in the upper cretaceous Khasib Formation of AHDEB oilfield in Iraq*. Master's thesis. Southwest Petroleum University. doi:10.27420/d.cnki.gxysc.2018.000372
- Xue, Z. A., Hu, Z. F., Xiao, Y. F., and Wu, Y. P. (2022). Logging evaluation method and application of strongly heterogeneous carbonate reservoir in Middle East. *Sci. Technol. Eng.* (07), 2654–2663. doi:10.3969/j.issn.1671-1815.2022.07.013
- Zhang, J. L., Hu, M. Y., Wang, A. Y., Zhang, B., Yan, B., and He, X. X. (2021). Sedimentary configuration and reservoir distribution in the Cambrian mound-shoal complexes at platform margins of Gucheng area, Tarim Basin. *Oil Gas Geol.* 03, 557–569. doi:10.11743/ogg20210303
- Zhang, W. Q., Liu, D. W., Zhang, L. F., Deng, Y., Xu, J. C., and Wang, Y. N. (2023). Characteristics and genetic mechanism of marine nodular limestone reservoirs of Khasib Formation in Iraq A Oilfield, Middle East. *Mar. Orig. Pet. Geol.* (01), 33–44. doi:10.3969/j.issn.1672-9854.2023.01.004
- Zheng, H. F., Yuan, L. L., Liu, B., Zhang, X. F., Shen, Y. C., and Wang, Y. C. (2020). Origins of dolomitization fluids within middle permian coarse dolomite, SW sichuan basin. *Acta Sedimentol. Sin.* (3), 589–597. doi:10.14027/j.issn.1000-0550.2019.046